Journal Pre-proof

Atorvastatin ameliorates diabetic nephropathy through inhibiting oxidative stress and ferroptosis signaling.

Yaoxia Zhang, Yuanyuan Qu, Ruiping Cai, Junjia Gao, Qian Xu, Lu Zhang, Mengjie Kang, Hui Jia, Qing Chen, Yueyang Liu, Fu Ren, Ming-Sheng Zhou

PII: S0014-2999(24)00387-X

DOI: https://doi.org/10.1016/j.ejphar.2024.176699

Reference: EJP 176699

To appear in: *European Journal of Pharmacology*

Received Date: 4 December 2023

Revised Date: 17 May 2024

Accepted Date: 28 May 2024

Please cite this article as: Zhang, Y., Qu, Y., Cai, R., Gao, J., Xu, Q., Zhang, L., Kang, M., Jia, H., Chen, Q., Liu, Y., Ren, F., Zhou, M.-S., Atorvastatin ameliorates diabetic nephropathy through inhibiting oxidative stress and ferroptosis signaling., *European Journal of Pharmacology*, https://doi.org/10.1016/j.ejphar.2024.176699.

Atorvastatin ameliorates diabetic nephropathy through inhibiting oxidative stress and ferroptosis signaling.

Yaoxia Zhang[1&2#], Yuanyuan Qu[1&2#], Ruiping Cai[2], Junjia Gao[3], Qian Xu[1], Lu Zhang[1], Mengjie Kang[1&2], Hui Jia[4], Qing Chen[4], Yueyang Liu[5], Fu Ren[6]*, Ming-Sheng Zhou[1,2]*

1. Science and Experiment Research Center & Shenyang Key Laboratory of Vascular Biology, Shenyang Medical College, Shenyang, China, 110034;
2. Department of Physiology, Shenyang Medical College, Shenyang, China, 110034;
3. Department of Cardiology, 2nd Affiliated Hospital, Shenyang Medical College 110000;
4. School of Traditional Chinese Medicine, Shenyang, China, 110034
5. Department of Pharmacy, Shenyang Medical College, Shenyang, China, 110034
6. Department of Anatomy, Shenyang Medical College, Shenyang, China, 110034

Running title: Statins therapy in diabetic nephropathy

Words of abstract: 250

Total word count: 8227

Number of figures: 10

***Corresponding Authors:**

Ming-Sheng Zhou, MD & Ph.D.,

Science & Experiment Research Center,

Shenyang Medical College, Shenyang, China.

Tel: +86-24-62215682, Fax: +86-24-62215656,

Email: zhoums@symc.edu.cn

Fu Ren MD & Ph D

Department of Anatomy

Shenyang Medical College,

Shenyang, China

Tel: +86-24-62215811, Fax: +86-62215656,

Email: rf@symc.edu.cn

 # equally contribute to the work.

Abstract

Clinically, statins have long been used for the prevention and treatment of chronic renal diseases, however, the underlying mechanisms are not fully elucidated. The present study investigated the effects of atorvastatin on diabetes renal injury and ferroptosis signaling. A mouse model of diabetes was established by the intraperitoneal injection of streptozotocin (50 mg/kg/day) plus a high fat diet with or without atorvastatin treatment. Diabetes mice manifested increased plasma glucose and lipid profile, proteinuria, renal injury and fibrosis, atorvastatin significantly lowered plasma lipid profile, proteinuria, renal injury in diabetes mice. Atorvastatin reduced renal reactive oxygen species (ROS), iron accumulation and renal expression of malondialdehyde (MDA), 4-hydroxynonenal (4-HNE), transferrin receptor1 (TFR1), and increased renal expression of glutathione peroxidase 4 (GPX_4), nuclear factor erythroid 2-related factor (NRF_2) and ferritin heavy chain (FTH) in diabetes mice. Consistent with the findings *in vivo*, atorvastatin prevented high glucose-induced ROS formation and Fe^{2+} accumulation, an increase in the expression of 4-HNE, MDA and TFR1, and a decrease in cell viability and the expression of NRF_2, GPX_4 and FTH in HK_2 cells. Atorvastatin also reversed ferroptosis inducer erastin-induced ROS production, intracellular Fe^{2+} accumulation and the changes in the expression of above-mentioned ferroptosis signaling molecules in HK_2 cells. In addition, atorvastatin alleviated high glucose- or erastin-induced mitochondria injury. Ferroptosis inhibitor ferrostatin-1 and antioxidant N-acetylcysteine (NAC) equally reversed the expression of high glucose-induced ferroptosis signaling molecules. Our data support the notion that statins can inhibit diabetes-induced renal oxidative stress and ferroptosis, which may contribute to statins protection of diabetic nephropathy.

Key words: Diabetic nephropathy, ferroptosis, oxidative stress, statins, diabetes, renal diseases

1. Introduction

Type II diabetes are prevalent worldwide. Approximately 20% of diabetes patients have diabetes kidney diseases (DKD), DKD is the leading cause of end-stage renal disease associated with increased incident dialysis rate, poor cardiovascular outcome and all-cause morbidity and mortality (Bolignano et al., 2017; Gruden et al., 2005; Mansi et al., 2021). DKD is a prototypical metabolic disorder of gene and environmental interactions. Hyperglycemia induces metabolic alterations, including mitochondrial dysfunction, glucose and fatty acid oxidation abnormalities, endoplasmic reticulum (ER) stress, and energy utilization changes, which may activate multiple cellular pathways, increasing oxidative stress, inflammation, cell death and proliferation(Lindblom et al., 2015; Samsu, 2021).

Ferroptosis is a new form of programmed cell death caused by iron-dependent accumulation of lipid peroxidation(Dixon et al., 2012). In the case of ferroptosis, overexpression of transferrin receptor 1 (TFR1) and low expression of ferritin heavy chain (FTH) may cause excessive accumulation of ferrous iron, which promotes massive production of reactive oxygen species (ROS) through the Fenton reaction, leading to the peroxidation of phospholipid-containing polyunsaturated fatty acids(Gao et al., 2019; Li et al., 2020). On the other side, the loss of the antioxidant capacity makes the lipid membranes of cells containing phospholipids vulnerable to ROS attack, forming the end products of lipid peroxidation, such as malondialdehyde (MDA) and 4-hydroxynonenal (4-HNE), resulting in cytotoxicity and cell ferroptosis(Ayala et al., 2014; Rochette et al., 2022).

Recent studies have suggested that ferroptosis involves in the pathogenesis of DKD(Huang and Yuan, 2024; Shen et al., 2022). Some changes related to ferroptosis, such as oxidative stress, excessive iron accumulation and lipid peroxidation products, are found in the kidney of diabetes

mice or DKD patients(Mengstie et al., 2023). Animal studies have shown that some agents, such as ferroptosis inhibitors or iron chelating agents, can slow down or prevent the progression of DKD(Feng et al., 2021). Therefore, some investigators propose that targeting ferroptosis may be a new approach for the prevention and treatment of DKD(Chen et al., 2024; Wu et al., 2022).

Statins or the hydroxymethylglutaryl coenzyme A (HMG-CoA) reductase inhibitors, are potent inhibitor of endogenous cholesterol synthesis. In addition to lowering lipids, statins are also endowed with pleiotropic effects, including antioxidant, inhibition of inflammation and upregulation of endothelial nitric oxide synthase (eNOS), which have beneficial effects on the cardiovascular and renal system(Bellosta et al., 2000). Statins have been shown to slow down the progression of atherosclerosis and promote the regression of atherosclerosis, and improve cardiovascular outcomes in humans with normal and elevated serum cholesterol levels(Orkaby et al., 2020; Zhang et al., 2020). We have previously shown that treatment with atorvastatin increases renal eNOS expression and reduces renal oxidative stress, inflammation, and fibrosis, thereby providing renal protection in hypertensive rats(Zhou et al., 2008).

Statins also play an important role in the treatment of diabetic nephropathy (Qin et al., 2017). Many randomized controlled trials confirm that the therapeutic effects of statins on diabetic nephropathy are more beneficial than harmful (Sandhu et al., 2006). However, some investigators have reported that chronic treatment with statins may increase the risk of insulin resistance in diabetes patients (Zigmont et al., 2019), and the effect of statin on diabetic nephropathy is still controversial (Huang et al., 2023; Shen et al., 2016; Zhou et al., 2014). In this study, we investigated whether statins can inhibit ferroptosis signaling and protect against renal injury in streptozotocin (STZ)/high fat diet-induced diabetes mice.

2. Materials and Methods

2.1 Materials and reagents

Atorvastatin was purchased from GLPBIO (Shanghai, China) , STZ was obtained from Sigma-Aldrich (St Louis, MO), 2,7-dichlorodihydrofluorescein diacetate (DCFH-DA) fluorescent probe assay kit was obtained from Beyotime Biotechnology (S0033S, Shanghai, China), FerroOrang was obtained from DOJINDO (F374, Japan), dihydroethidine (DHE) was purchased from Med Chem Express LLC (Shanghai, China), and the primary antibodies were purchased from following companies: anti-glutathione peroxidase4 (GPX_4), anti-4-HNE, anti-TFR1 and anti-MDA antibodies (Abcam, Inc.), anti-FTH(Cell Signaling Technology, Inc.) antibody, anti-β-actin anti-body (ProteinTech Group, Inc.), and anti- nuclear factor erythroid 2-related factor 2 (NRF_2) antibody (Abmart, Inc.), anti-p22phox, anti-gp91phox, anti-transform growth factor 1 （TGFβ1）and anti-fibronectin antibodies (Santa Cruz Biotechnology, Inc.).

2.2 Animal protocols:

The 8-weeks-old male C57BL/6 mice were purchased from Changsheng Biotechnology (Benxi, China). All animal protocols were implemented in accordance with the institute's guidelines for animal care and use, and had been approved by the Animal Care and Use Committee of Shenyang Medical College (SYYXY2021032301, Shenyang, China). Mice were housed in a pathogen-free animal facility at Shenyang Medical College with free access to mouse chow and tap water. Mice were allowed to adapt to the new environment for 2 weeks. To induce type II diabetes, the mice were injected intraperitoneally with STZ at a dose of 50 mg/day/kg body weight for 5 consecutive days, while control mice were injected intraperitoneally with the same volume of citrate solution. The mice at STZ group or STZ plus atorvastatin group were fed a high-fat diet (45% caloric from fat, Medicience Ltd. Yangzhou, China) 10 days before the intraperitoneal injection of STZ, until

the end of the experiments. The mice at control group were fed a normal fed diet (17% caloric from fat). Fasting blood glucose level > 250 mg/dl is considered as the criterion of successful diabetes model. After the establishment of diabetes model, diabetes mice were divided into diabetes group (STZ) and atorvastatin (AT) treated diabetes group. AT group mice were given atorvastatin at the dose of 30 mg/day/kg body weight by gavage for 8 weeks, the experimental protocols were shown in figure 1A. Body weight was measured weekly, and fasting blood glucose was measured biweekly by an automatic blood glucose meter (Roche Accu-CHEK Active, Mannheim, Germany). Urine was collected by squeezing the mouse bladder on a metal plate to stimulate urination. Urine albumin was measured by Bio-Rad protein assay (Beyotime Biotech., Shanghai, China), urine creatinine was determined using creatinine assay kit (Nanjing Jiangchen Bioengineering Institute Co., Nanjing, China) according to the manufacturer's instructions, urine albumin excretion was expressed as the ratio of albumin to creatinine. At the end of the study, mice were fasted overnight and anesthetized with a mixture of 100 mg/kg ketamine and 20 mg/kg xylazine, the chest of the mice was immediately opened, and blood was harvested through left ventricular puncture. Blood samples were used for determining plasma levels of total cholesterol (TC) and total triglycine (TG), urea nitrogen (BUN). The kidneys were collected and snap frozen in liquid nitrogen.

2.2 Renal histological analysis

Kidney tissue was fixed with 4% paraformaldehyde in PBS and embedded in paraffin, and cut into 4 μm thick section. Periodic Acid Schiff (PAS) staining was used to evaluate glomerular and tubular injury, including the glomerular sclerosis and the dilation of the mesangial matrix. The images were taken using an Olympus DP-72 camera in the Olympus DS-41 microscope (Olympus, Japan). Five images with total of 10 glomeruli per sample were examined in a blind manner. Glomerular sclerosis (a dark purple color in glomerular area) was quantified with ImageJ software, the percentage of glomerular sclerotic area with total glomerular areas for 10 glomeruli was

measured and averaged as a single measurement. Masson-trichrome staining was used to evaluate renal fibrosis. Renal collagen was analyzed with ImageJ software and expressed as percentage positive stained areas with total stained areas.

2.3 Determination of renal tissue iron content

Renal tissue iron content was assayed using an iron assay kit according to manufacturer's instructions (Cat#: A039-2-1, Jiancheng Bioengineer Institute, Nanjing, China). Briefly, renal tissue (about 80 mg, 1:9 dilution) was homogenized with physiological saline solution, and centrifuged at 3500 rpm for 10 min. The supernatant was taken, and added 0.5 ml supernatant and 1.5 ml ferrous assay buffer solution in tube to mix well, the mixed solution was boiled for 10 min, and centrifuged at 3500 rpm for 10 min. The supernatant was taken, and added 200 μl supernatant into 96 well plates. Iron content was detected by spectrophotometer (Omega, Germany) at 510 nm, tissue iron concentration was calculated by iron standard curve and normalized with per gram tissue protein.

2.4 Western blot

Kidney tissues were homogenized with lysis buffer containing 1 mmol/L PMSF, 10 μg/ml aprotinin and 10 μg/ml leupeptin. Protein concentration was measured by Bio-Rad protein assay kit (California, USA). Thirty μg of protein were separated by SDS-PAGE, and transferred to a nitrocellulose membrane. After blocking with a 5% milk/TBS blocking solution, the membranes were incubated with primary antibodies at 4^{o}C overnight, primary antibodies include anti-GPX_4 (1:1,000; cat. no. 125066), anti-FTH (1:1,000; cat. no. 4393), anti-4-HNE (1:1,000; cat. no.46545), anti-TFR1 (1:2,000; cat. no.214039), anti-MDA (1:1,000; cat. no.27642) and anti-NRF_2 (1:1,000; cat. no. T551365), anti-p22phox (1:1,000; cat. no.271262), anti-gp91phox (1:1,000; cat. no.130543), anti-TGFβ1(1:1,000; cat. no.130348), anti-fibronectin (1:1,000; cat. no.271098)

antibodies. The membranes were washed three times with TBS, then incubated with the secondary antibody conjugated with horseradish peroxidase at room temperature for one hour. The immunoblots were visualized by enhanced chemiluminescence (ECL, Santa Cruz Biotech. Inc.), which were detected by an Aplegen Omega Lum G Gel Documentation System (Aplegen Inc., Pleasanton), densitometric analyses were quantified by ImageJ. 1.48V software system. β-actin (1:10,000; cat. no. 66009-1-Ig) was used as a loading control, and data was expressed as fold increase versus control group.

2.5 Determination of renal reactive oxygen species (ROS) production with fluorescent dihydroethidine (DHE) staining.

Oxidative fluorescent dye DHE was used to determine the renal O_2^- production as described in our previous publications (Huang et al., 2018). In briefly, fresh renal tissues were embedded in OCT compound and snap frozen with liquid nitrogen. Four μm thickness of renal sections were cut with microtome-cryostat. Sections were incubated with 2 μmol/L DHE in HEPES buffer for 30 minutes at 37 ^oC. At least 5 images per section were taken using a laser scanning confocal fluorescence microscope, and average oxidative fluorescent intensity was quantified.

2.6 Immunohistochemistry analysis

Renal sections (4 μm) were cut from paraffin embedded tissues for immunofluorescence analysis. After deparaffinization and hydration, renal sections were microwaved for 30 minutes at 60 ^oC for antigen retrieval. The sections were incubated with the primary antibodies against MDA (1:200 dilution with PBS buffer; cat. no.27642) and 4-HNE (1:200 dilution with PBS buffer; cat. no.46545) overnight at 4 ^oC, followed by the incubation with HRP labeled streptavidin for 15 min at room temperature and stained with DAB solution. The section without the incubation with primary antibody was used as a negative control. The nuclei were counter-stained with DAPI. Images were acquired by a Leica DM4B fluorescence microscope (Leica Microsystems Inc.,

Mannheim, Germany) and analyzed with ImageJ version 1.48 software. Results were expressed as a percentage of positive stained areas with total selected areas.

2.7 Cell culture

Human renal epithelial (HK_2) cells were cultured in DMEM medium containing 10% FBS, streptomycin (100 mg/ml) and penicillin (100 U/ml) under a humidified atmosphere of 5% CO_2 at 37 °C. Cells were cultured with normal glucose (NG, 5.5 mmol/L D-glucose), high mannitol (24.5 mmol/L D-mannitol plus 5.5 mmol/L D-glucose, HM), high glucose (HG, 30 mmol/L D-glucose), and HG plus atorvastatin treatment (AT, 10 μmol/L) for 24 hours. Mannitol group was used for controlling cell osmolality. In some experiments, HK_2 cells were treated with erastin (ferroptosis inducer, 10 μmol/L), ferrostatin-1 (ferroptosis inhibitor, 10 μmol/L) with or without atorvastatin (10 μmol/L).

2.8 Measurement of intracellular ROS

Intracellular ROS production was measured by 2,7-dichlorodihydrofluorescein diacetate (DCFH-DA) fluorescent probe assay kit according to the manufacturer's instructions (S0033S, Beyotime Biotechnology, Shanghai, China). Briefly, HK_2 cells were seeded into a 24 well plate for 24 hours. Cells were incubated with 10 μmol/L DCFH-DA without light at 37 °C for 30 minutes, washed with PBS three times, and DCF fluorescence intensity and areas of each cell in the viewed field were measured using a fluorescence microscope (Leica, Germany), and the total fluorescence intensity and total areas of cells were calculated. The mean fluorescence intensity was obtained by dividing the total fluorescence intensity of cells by the total cell areas and subtracting the background fluorescence intensity. Data was expressed as pixels/μm^2.

2.9 Determination of cell viability

HK_2 cell viability was determined using the CCK-8 assay kit according to the manufacturer's instruction (Vazyme, A311-01, Nanjing, China). In brief, HK_2 cells were diluted to 2×10^4 cells and seeded in 96-well plates (6×10^3 cells/well) and treated with NG, HM, HG or HG plus AT for 24 hours. Then culture medium was replaced with 100 μl fresh medium supplemented with 10 μl of the CCK-8 solution and incubated for 2 hours at 37°C, absorbance at 450 nm was measured with a microplate reader (Omega, Germany). PBS without cells was used as blank control. Each sample was run in 3 wells (triplet), and the average of three wells is taken as a single measurement.

2.10 Transmission electron microscopy（TEM）

HK_2 cells were fixed in 2.5% glutaraldehyde in PBS and postfixed with 1% osmic acid solution. Cells were followed by dehydration in graded ethanol, and embedded in epoxy resin embedding medium. Ultra-thin (90 nM) sections were placed on uncoated copper grids, and stained with 2% uranyl acetate and 0.1% lead citrate. The grids were examined and photographed using TEM operating at 80 kV (HITACHI, H-7650, Japan）.

2.11 Determination of intracellular Fe^{2+} concentration with FerroOrange fluorescence staining

HK_2 cells were stained with 1 mmol/L FerroOrang (DOJINDO, F374, Japan) in Hanks' balanced salt solution at 37℃ for 30 minutes in the dark, then fluorescent-stained cells were observed with a fluorescence microscope. Average fluorescence intensity was measured using imageJ software and calculated by dividing the total fluorescence intensity of cells by the total cell areas and subtracting the background fluorescence intensity. Data was expressed as pixels/μM^2.

2.12 Statistical analysis

Results were expressed as mean ± SD of independent animal or cell-based experiments.

Statistical analyses were performed by one-way ANOVA with Tukey's multiple comparison. Values were considered significant when $p< 0.05$.

3. Results

3.1 Atorvastatin lowers plasma lipid profile and improves renal function in STZ/high fat diet-induced diabetes mice

Compared with control mice, fasting blood glucose in STZ mice treated with high fat diet (STZ/HF) significantly increased (17.4 ± 0.7 vs. 3.9 ± 0.5 mmol/L in control mice, p<0.05, Figure 1B), indicating a successful model of mouse diabetes. STZ/HF-induced diabetes mice had higher fasting plasma total cholesterol and total triglyceride, and lower body weight (Figures 1C-E, all

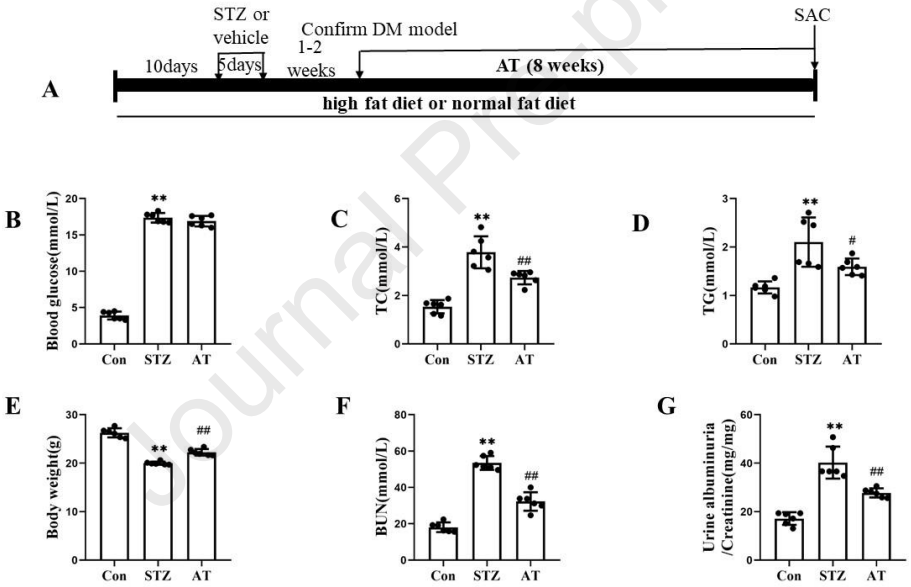

Figure 1. Atorvastatin treatment reduces plasma lipid profile and renal function in streptozotocin（STZ) with high fat diet (HF)-induced diabetes mice. A: a schematic diagram of experimental protocols. B: fasting plasma glucose; C: fasting plasma total cholesterol (TC); D: fasting plasma total triglyceride (TG); E: body weight; F: plasma urea nitrogen (BUN), G: urine albumin excretion. Con: control mice; STZ; streptozotocin with high fat diet-induced diabetes mice; AT: diabetes mice treated with atorvastatin. Data was expressed mean ± SD, n=6, **p<0.01 vs. control mice, $^{\#}$p<0.05 & $^{\#\#}$p<0.01 vs. diabetes mice.

p<0.05). Treatment with atorvastatin significantly lowered lipid profile, and slightly increased body weight (p<0.05), but had not significant effect on plasma glucose. Plasma BUN and urine albumin excretion significantly increased in diabetes mice (all p<0.05, Figures 1F-G), and atorvastatin significantly reduced plasma BUN and albuminuria in diabetes mice.

3.2 Treatment with atorvastatin lowers renal injury and fibrosis in diabetes mice

We evaluated the effects of atorvastatin on renal injury and fibrosis using PAS staining and

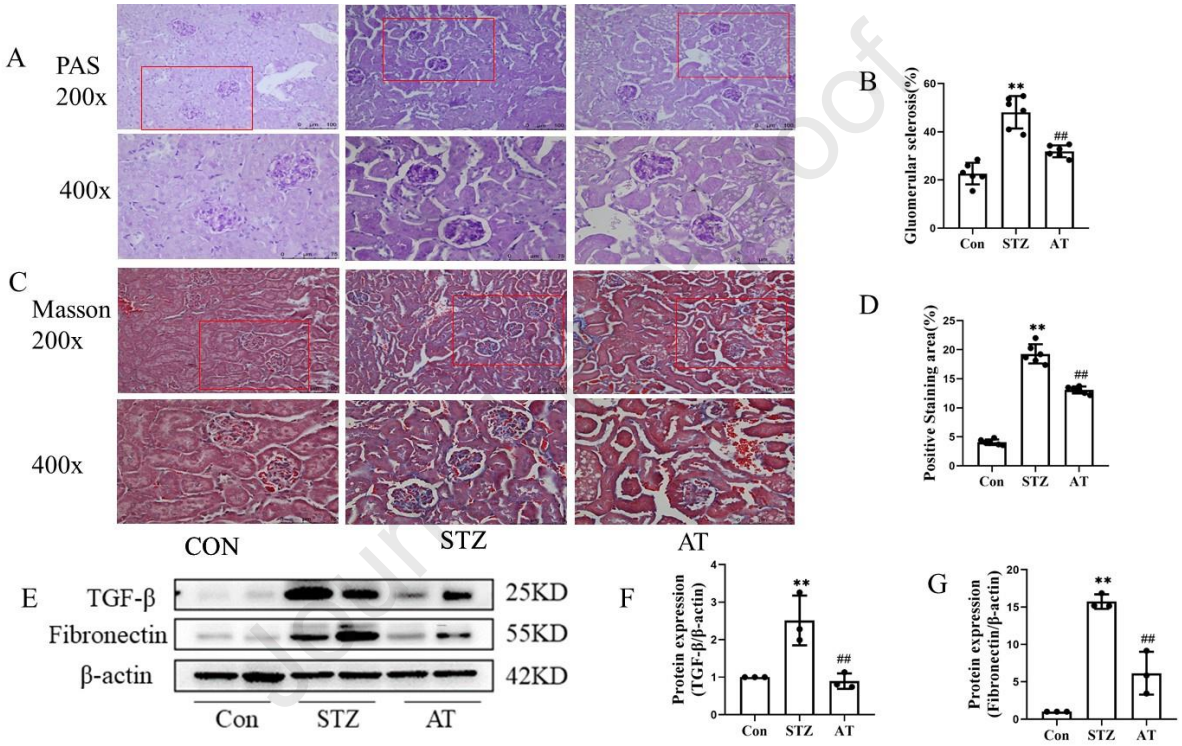

Figure 2. Atorvastatin treatment protects against renal injury and fibrosis in diabetes mice. A: Representative images of renal sections stained with periodic acid-Schiff (PAS) to evaluate renal morphological injury, top pane: 200x magnification, low pane: 400x magnification; B: Quantitation of glomerular sclerosis and injury; C: Representative renal images stained with Masson trichrome for evaluation of renal fibrosis, top pane: 200x magnification, low pane: 400x magnification; D. Quantification of renal positive collagen staining areas; n=6. Representative image bands (E) and semi-quantitation of the protein expression of transforming growth factor (TGFβ) (F) and fibronectin (G); n=3, **p<0.01 vs. control mice, $^{\#\#}$p<0.01 vs. diabetes mice.

Masson-trichrome staining, respectively. PAS staining showed that diabetes mice had obvious glomerular and renal tubule injury, which manifested by increased glomerular sclerotic area, glomerular mesangial expansion and renal tubular atrophy. Atorvastatin treatment reduced diabetes-induced renal glomerular and tubular injury (Figures 2A&B). Masson-trichrome showed that diabetes mice had more collagen positive staining areas than control mice, which significantly reduced in atorvastatin-treated mice (Figures 2C&D). We determined renal protein expressions of fibrotic factors TGFβ and fibronectin, the protein expression of TGFβ and fibronectin significantly increased in diabetes mice, treatment with atorvastatin reduced the expressions of these fibrotic proteins (Figures 2E-G).

3.3 Atorvastatin attenuates renal oxidative stress in diabetes mice.

We determined renal ROS generation by DHE fluorescent staining and the protein expression

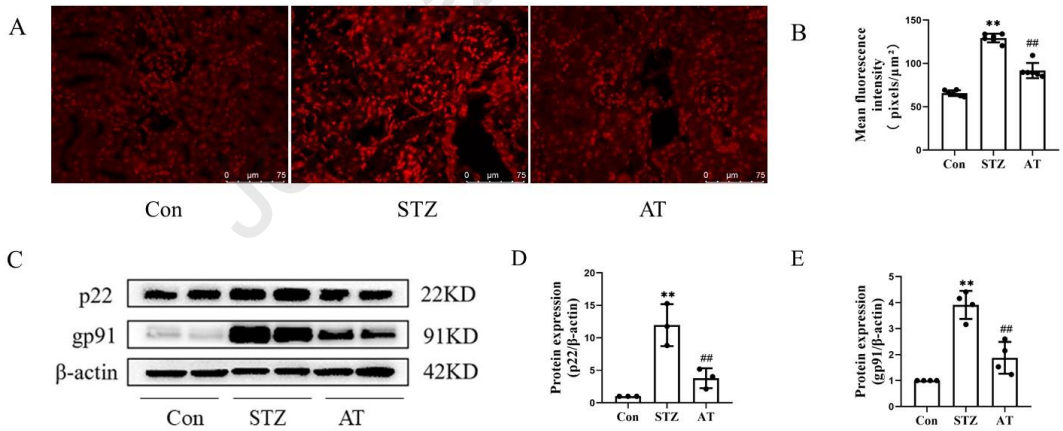

Figure 3. Atorvastatin reduces renal oxidative stress in diabetes mice. A: Representative renal images stained with DHE oxidative fluorescence, n=6; B: Quantification of average oxidative fluorescence intensity; The representative image bands (C) and semi-quantitation of protein expressions of NADPH oxidative subunits p22phox (D) and gp91phox (E). n=3, **p<0.01 vs. control mice; ##p<0.01 vs. diabetes mice.

of NADPH oxidase subunits of gp91phox and p22phox. Average oxidative fluorescent density significantly increased in the kidney of diabetes mice, which was prevented by atorvastatin

treatment (Figures 3A-B). Renal protein expression of gp91phox and p22phox significantly increased in diabetes mice, atorvastatin treatment reduced the protein expression of gp91phox and p22phox (Figures 3C-E).

3.4 Atorvastatin reverses renal protein expression of ferroptosis signaling molecules in diabetes mice.

NRF_2 is an important transcription factor, and GPX_4 is a downstream molecule of NRF_2(Xu et al., 2021). It has been shown that the activation of NRF_2/GPX_4 inhibits ferroptosis inducer RSL3-

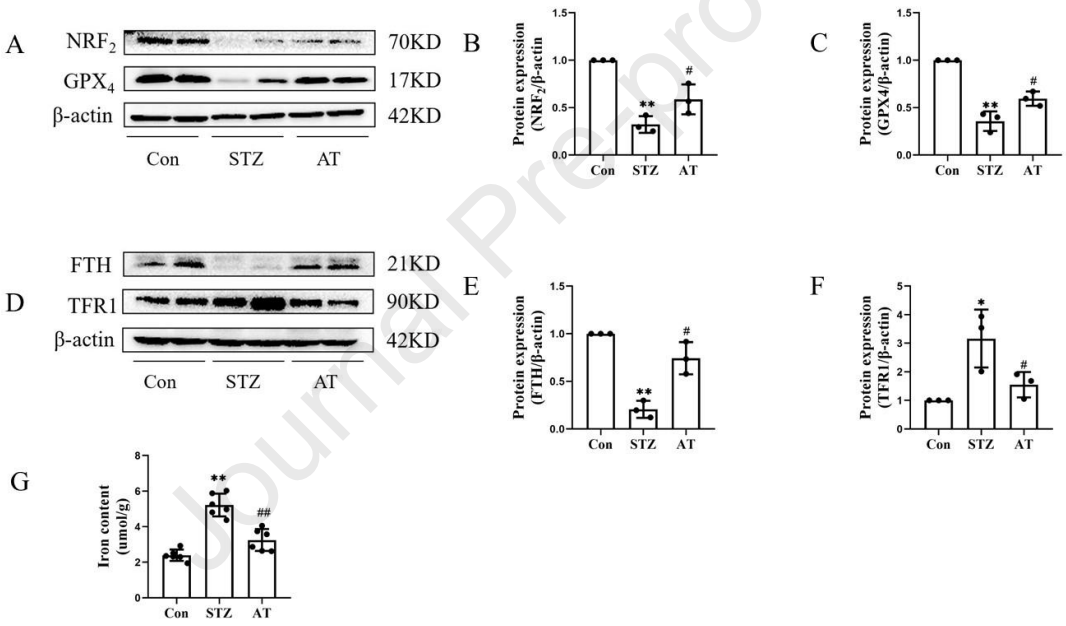

Figure 4. Atorvastatin reverses renal expression of ferroptosis signaling molecules and reduces renal ferrous accumulation in diabetes mice. The representative image bands (A) and semi-quantitation of the protein expression of nuclear factor erythroid 2-related factor (NRF_2, B), glutathione peroxidase 4 (GPX_4, C); The representative image bands (D) and semi-quantitation of the protein expression of ferritin H (FTH, E) and transferrin receptor 1 (TFR1, F), n=3. G: renal tissue iron concentration. n=6, *$p<0.05$ &**$p<0.01$ vs. control mice, $^{\#}p<0.05$ & $^{\#\#}p<0.01$ vs. diabetes mice.

induced ferroptosis(Liao et al., 2022). As shown in figures 4A-C, the protein expression of NRF_2 and GPX_4 significantly reduced in the kidney of diabetes mice, which increased in atorvastatin-treated diabetes mice. FTH is a downstream molecule of NRF_2 and has anti-ferroptosis effect. FTH expression reduced in the kidney of diabetes mice, atorvastatin treatment increased FTH expression (Figures 4D&E). The renal protein expression of TFR1 significantly increased in diabetes mice, which prevented by atorvastatin treatment (Figures 4D&F). Iron content in renal tissue significantly increased in diabetes mice, which also reduced in atorvastatin-treated diabetes mice (Figure 4G). Ferroptosis is charactered with iron-dependent lipid peroxidation, MDA and 4-HNE are two important markers of lipid oxidative damage in cell membrane. Semi-quantitation with immunohistochemistry showed that the positive staining areas of MDA and 4-HNE significantly increased in renal section of diabetes mice, and treatment with atorvastatin reduced MDA and 4-

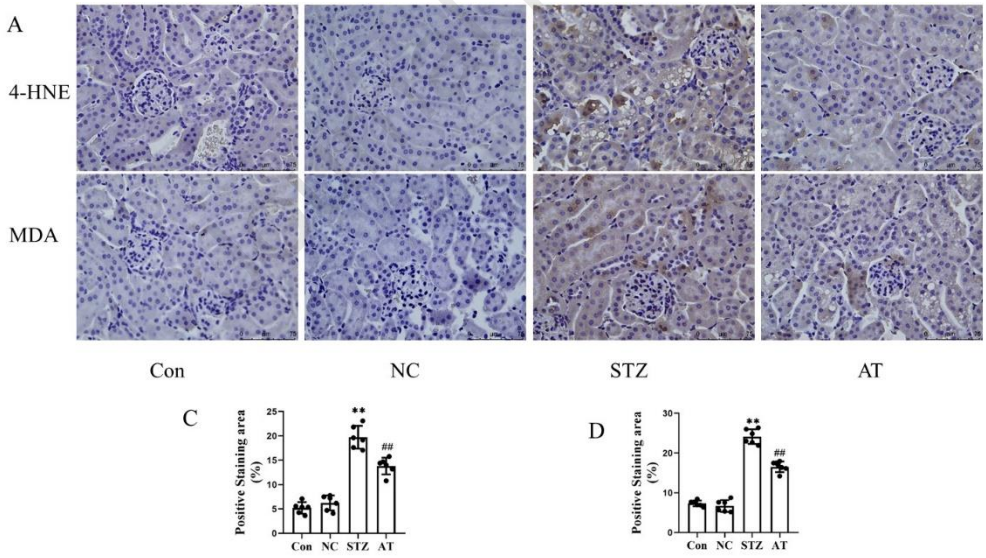

Figure 5. Atorvastatin reduces the expression of lipid peroxidation markers 4-Hydroxynonenal (4-HNE, A&C) and malondialdehyde (MDA, B&D) in diabetes mice. The representative images of 4-HNE (A) and MDA (B) assessed by immunohistochemistry, quantification of 4-HNE (C) and MDA (D). n=6, **p<0.01 vs. control mice, ##p<0.01 vs. diabetes mice.

HNE expressions in diabetes mice (Figure 5). The results suggest that atorvastatin could inhibit diabetes-induced renal ferroptosis signaling.

3.5 Atorvastatin inhibits erastin-induced oxidative stress and reverses the expression of ferroptosis signaling molecules in HK_2 cells.

It has been shown that erastin can induce oxidative stress and ferroptosis in various cells through the depletion of glutathione and the inhibition of GPX_4 (Gaschler et al., 2018). To determine the effects of atorvastatin on erastin-induced oxidative stress and ferroptosis signaling, HK_2 cells were treated with ferroptosis inducer erastin (10 μmol/L) with or without atorvastatin

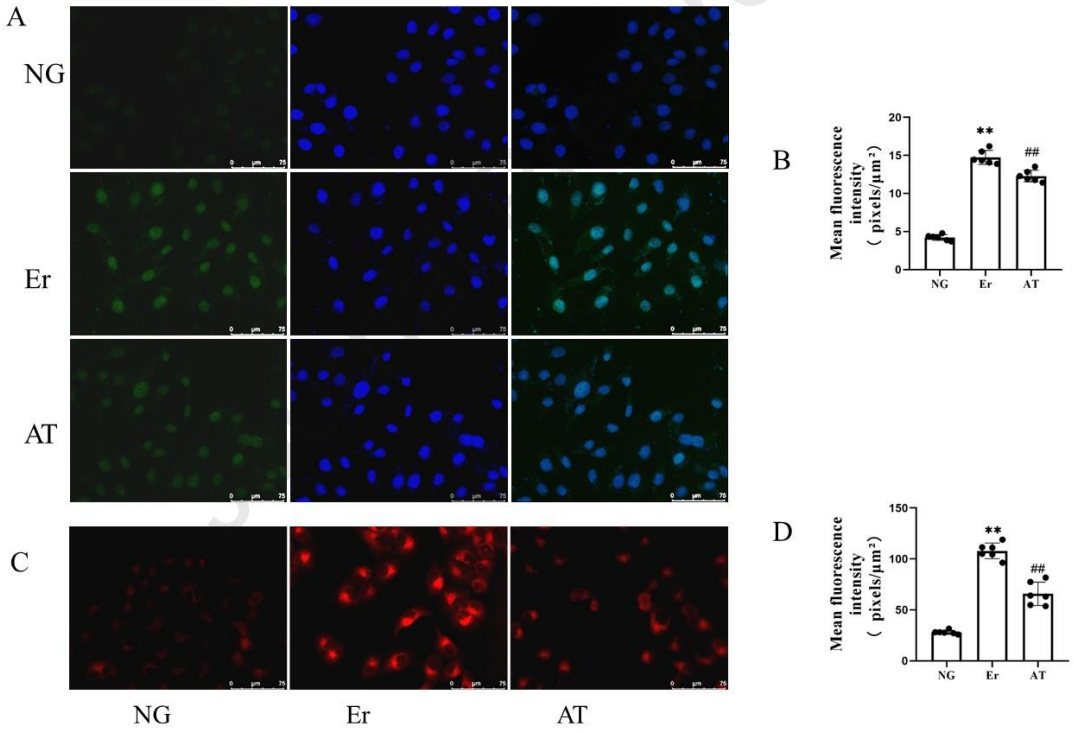

Figure 6. Atorvastatin decreases erastin-induced oxidative stress and intracellular Fe^{2+} accumulation in HK_2 cells. Erastin is a ferroptosis inducer. A: Representative images of reactive oxygen species fluorescence assessed by DCFH-DA staining; B: Quantification of ROS fluorescence intensity; C: Representative images of intracellular accumulation of Fe^{2+} (Red) stained with FerroOrange fluorescence; D: Quantification of FerroOrange fluorescence intensity. NG: normal control group, Er: erastin-treated group, AT: erastin plus atorvastatin treated group. n=6, **p<0.01 vs. control group, $^{\#\#}$p<0.01 vs. erastin group.

treatment (10 μmol/L). DCFH-DA fluorescence assay was used to determine the effect of atorvastatin on erastin-induced ROS production. Erastin significantly increased DCF oxidative fluorescence intensity, which reduced by atorvastatin treatment (Figures 6A&B). Intracellular iron overload is a characteristic of ferroptosis. We used ferroOrange probe to determine intracellular Fe^{2+} concentration. As shown in figures 6C&D, erastin treatment significantly increased

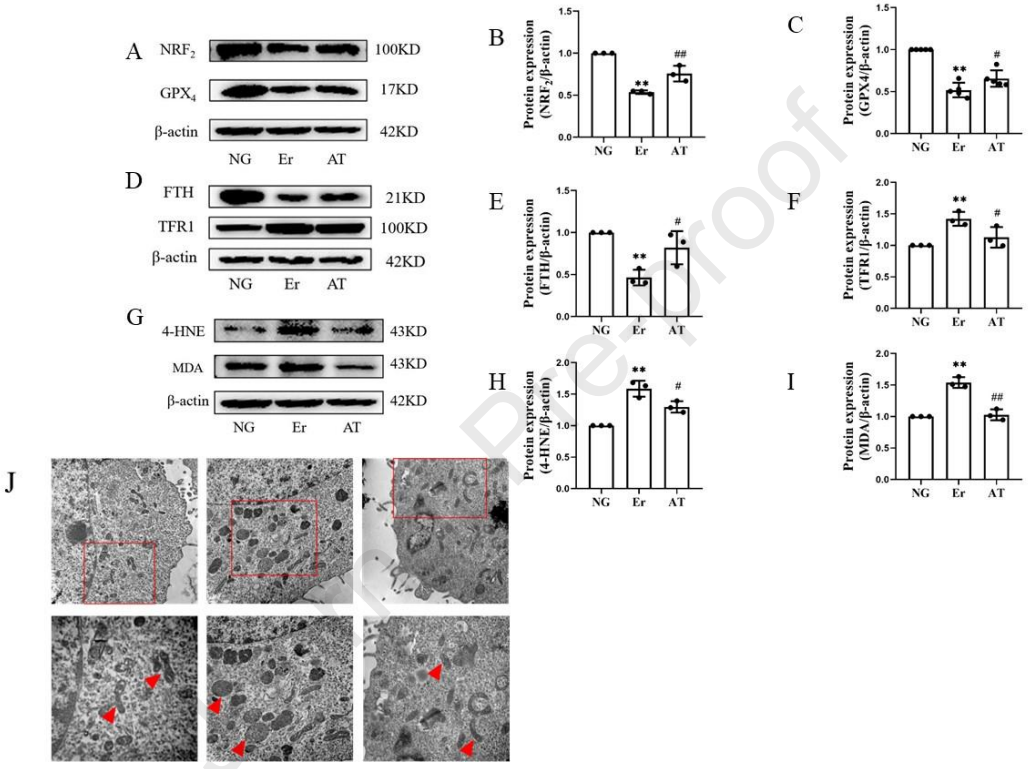

Figure 7. Atorvastatin reverses the expression of erastin-induced ferroptosis signaling molecules in HK_2 cells. Atorvastatin increased the protein expression of antioxidant genes NRF_2, GPX_4 and FTH, decreased TFR1 and lipid peroxidation markers MDA and 4-HNE in erastin-treated HK2 cells. The representative image bands of the protein expression of NRF_2 and GPX_4 (A), TFR1 and FTH (D), 4-HNE and MDA (G); the semi-quantitation of the protein expression of NRF_2 (B), GPX_4 (C), TFR1 (E), FTH (F), 4-HNE (H) and MDA(I); Atorvastatin improved mitochondria morphological damage and quantity induced by erastin (J). NG: normal control group, Er: erastin-treated group, AT: erastin plus atorvastatin treated group. Red arrow indicates mitochondria morphology changes in NG, Er and AT groups. n=3, $^{**}p<0.01$ vs. control group, $^{\#}p<0.05$ & $^{\#\#}p<0.01$ vs. erastin group.

intracellular ferroOrange fluorescence intensity, which markedly reduced in atorvastatin-treated cells. Furthermore, we determined the protein expression of antioxidant genes NRF_2 and GPX_4 (Figures 7A-C), iron metabolism related genes FTH and TFR1 (Figures 7D-F), and oxidative lipid damage markers 4-HNE and MDA (Figure 7 G-I). Erastin significantly decreased the expression of NRF_2, GPX_4 and FTH, while increasing the expression of TFR1, 4-HNE and MDA. Atorvastatin prevented erastin-induced changes in these molecules. Mitochondrial morphology is important for characterizing ferroptosis, we observed mitochondrial morphology in erastin-treated cells using TEM, as shown in figure 7J, erastin treatment induced mitochondria swelling or shrinkage, disappearance of mitochondria cristae, and reduction in the number of mitochondria, which is consistent with the characteristics of ferroptosis. Atorvastatin treatment reversed these changes. These results suggest that atorvastatin can reverse erastin-induced ferroptosis signaling and mitochondria morphology changes in HK_2 cells.

3.6 Atorvastatin inhibits glucose-induced oxidative stress and reverses the expression of ferroptosis signaling molecules in HK_2 cells

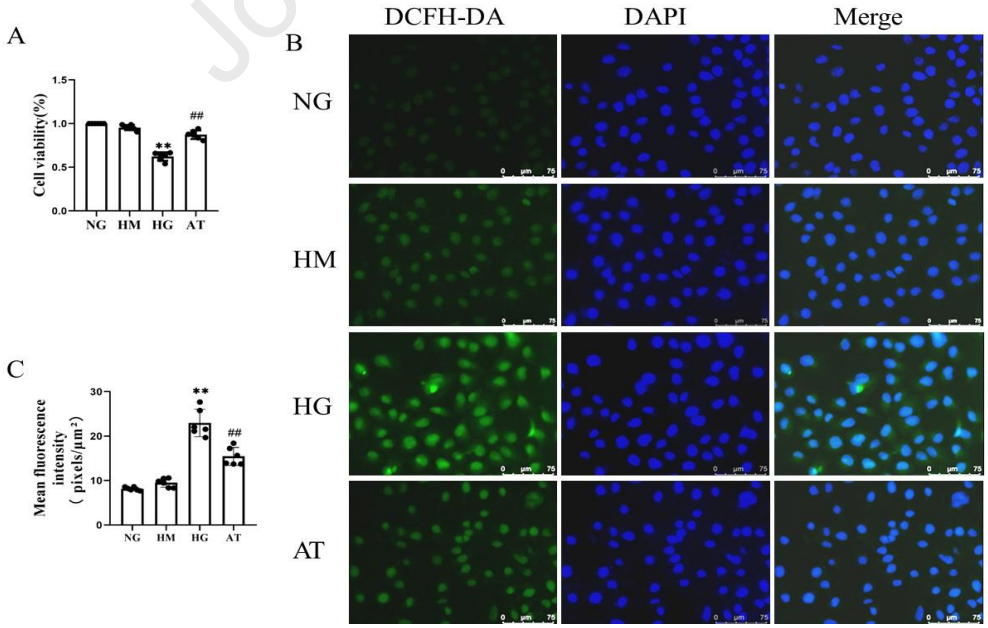

Figure 8. Atorvastatin increases cell viability and inhibits high glucose-induced oxidative stress in HK_2 cells. A: Cell viability assessed by CCK8 assay; B: Representative images of reactive oxygen species fluorescence assessed by DCFH-DA staining; C: Quantification of ROS fluorescence intensity. NG: normal glucose control group; HM: high mannitol (osmolarity control); HG: high glucose group; AT: high glucose with atorvastatin treatment group. n=6, **p<0.01 vs. control group, ##p<0.01 vs. HG group.

HK_2 cells were incubated with NG, HM, HG or HG plus AT for 24 hours. HG significantly reduced cell viability (Figure 8A) and increased oxidative fluorescence intensity (Figures 8B&C). Atorvastatin treatment increased cell viability and decreased oxidative fluorescence intensity in high glucose-treated cells. High glucose decreased the protein expression of GPX_4, NRF_2 and FTH (figure 9A-E), and increased the protein expression of TFR_1, 4-HNE and MDA （Figure 9D, F-I）, which were reversed by atorvastatin (Figure 9). We used TEM to examine mitochondrial

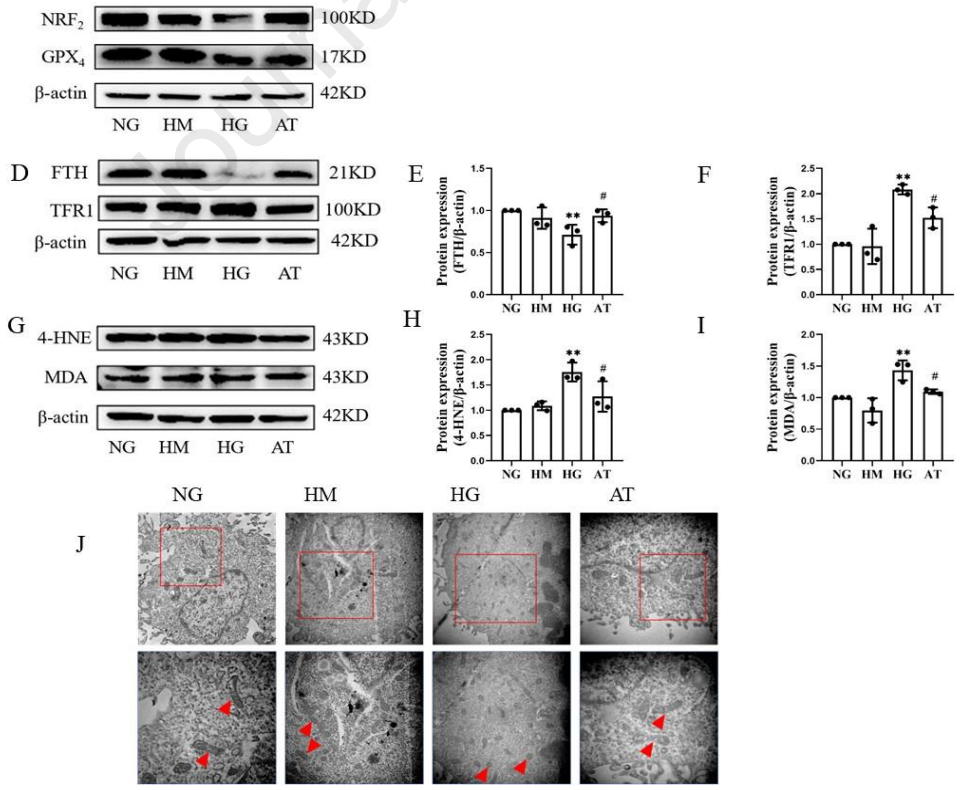

Figure 9. Atorvastatin reverses the expression high glucose-induced ferroptosis molecules in HK_2 cells. The representative image bands of GPX_4 and NRF_2 (A), FTH and TFR1 (D), 4-HNE and MDA (G); the semi-quantitation of the protein expression of NRF_2 (B), GPX4 (C), FTH (E), TFR1 (F), 4-HNE (H) and MDA(I), atorvastatin improved mitochondria morphological damage and quantity induced by HG (J). Red arrow indicates mitochondria morphology changes in NG, HM, HG and AT groups. n=3, *p<0.05 &**p<0.01 vs. NG group, #p<0.05 vs. HG group.

morphology, as shown in figure 9J, high glucose-induced changes in mitochondrial morphology were similar to those induced by erastin, including mitochondria slender and shrinkage, disappearance of mitochondria cristae and a decrease in the number of mitochondria, atorvastatin treatment reversed these changes in mitochondria morphology.

3.7. Ferroptosis inhibitor ferostatin-1 and antioxidant NAC reduce high glucose-induced ROS formation and reverse ferroptosis signaling in HK_2 cells.

Ferrostatin-1 is the first synthetic ferroptosis inhibitor in the literature (Dixon et al., 2012). Here we investigated and compared the effects of ferrostatin-1 and antioxidant NAC on high glucose-induced ROS formation and ferroptosis signaling molecules. High glucose significantly increased

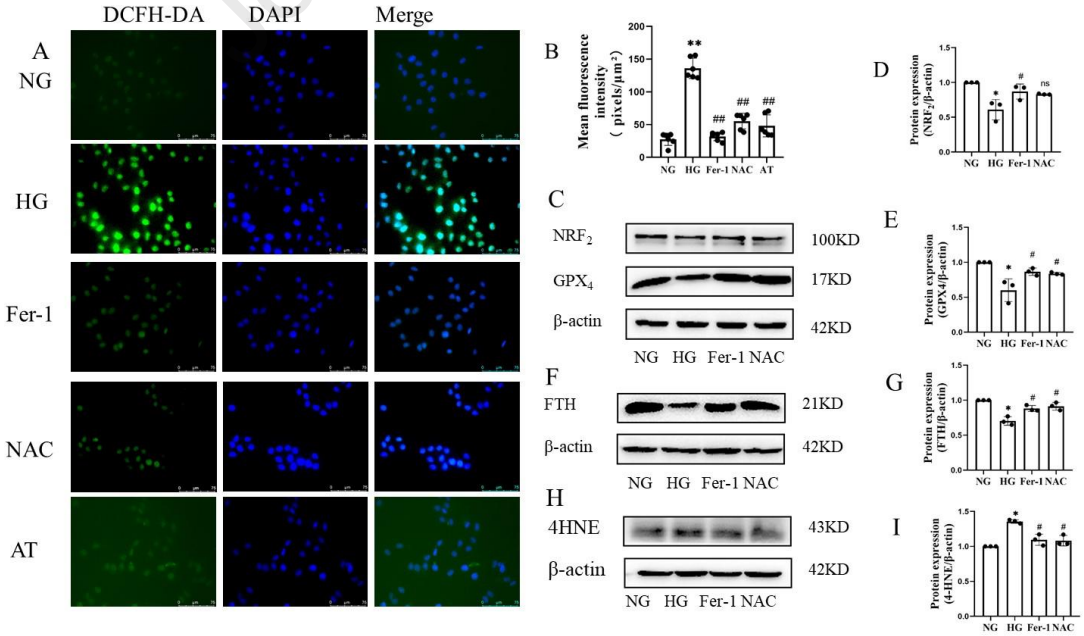

Figure 10. Effects of ferrostatin-1 (Fer-1) and NAC on high glucose-induced ROS formation and the expression of ferroptosis signaling molecules in HK_2 cells. Representative images of oxidative fluorescence stained by oxidative fluorescence DCFH-DA (A), atorvastatin, ferrostatin-1 and NAC significantly reduced high glucose-induced oxidative fluorescence intensity (B). The representative image bands of NRF2 &GPX4 (C), FTH (F) and 4HNE (H), the quantitation of the protein expression of NRF_2(D), GPX_4(E), FTH (G) and 4HNE (I). n=3, *p<0.05 &**p<0.01 vs. NG group, $^{\#}$p<0.05 & $^{\#\#}$p<0.05 vs. HG group.

oxidative fluorescence intensity, atorvastatin, ferostatin-1 and NAC have similar effects on reduced oxidative fluorescence intensity induced by high glucose (figures 10A&B). Furthermore, both ferostatin-1 and NAC prevented high glucose-induced decrease in the expression of NRF2, GPX4 and FTH (figure 10 C-G) and increase in 4-HNE expression (Figures H&I).

4. Discussion

The major findings of this study include: 1) Treatment with atorvastatin has a significant renoprotective effect in STZ/HFD-induced diabetes mice. Atorvastatin lowers proteinuria, glomerular and renal tubular injury, and fibrosis; 2) Our *in vivo* and *in vitro* studies show that atorvastatin has a potent antioxidant effect and inhibits ferroptosis signaling in diabetes kidney and HK_2 cells. Atorvastatin lowers renal ROS generation and the expression of oxidative lipid damage markers, and increases the antioxidant capacity, and reverses the expression of ferroptosis signaling molecules in diabetes mice and high glucose-treated HK_2 cells. In addition, atorvastatin inhibits erastin-induced ferroptosis in HK_2 cells. These results confer that statins have renal beneficial effects, the underlying mechanisms may involve antioxidant activity and the inhibition of renal cell ferroptosis signaling.

Statins have long been used for the primary and secondary prevention and treatment of chronic renal diseases (including DKD), the renoprotective effects of statins have been observed in several large clinical trials, such as CTT, DALI, WOSCOPS and CARDS(Baigent et al., 2011; Barayev et

al., 2023; Cholesterol Treatment Trialists et al., 2016). Diabetes is invariably associated with hyperlipidemia, which may promote lipid deposition in renal tubular and podocytes to cause lipotoxicity and renal injury(Battisti et al., 2003; Chen and Tseng, 2013). Statins are effective lipid-lowering agents, and are considered as first-line treatment for hyperlipidemia in diabetes and DKD(Cholesterol Treatment Trialists et al., 2016; Deng et al., 2015). In addition, DKD increases the risk for cardiovascular diseases, and the clinical application of statins is primarily employed for reducing blood cholesterol and preventing DKD-associated cardiovascular outcome(Colhoun et al., 2009). In addition to the lipid-lowering-dependent renoprotective effects, statins also have pleiotropic renoprotection which is lipid-lowering-independent in DKD patients or mice. These lipid-lowering-independent renoprotective effects include the inhibition of renal inflammation, proliferation, oxidative stress, and increased renal eNOS(Deng et al., 2015).

In our study, treatment with atorvastatin significantly reduces plasma cholesterol and triglycine, improves renal function, and lowers glomerular and renal tubular injury and fibrosis in diabetes mice. These results support the notion that clinical application of statins provides renoprotective effects in the patients with DKD. Furthermore, our results show that atorvastatin reduces renal ROS production, increases antioxidant capacity and inhibits renal cell ferroptosis signaling in DKD mice.

Oxidative stress plays an important role in the pathogenesis of DKD(Ostergaard et al., 2020; Winiarska et al., 2021). Hyperglycemia is a key factor for the development of DKD, hyperglycemia increases ROS generation in renal cells through diverse pathways, including the activation of NADPH oxidase, mitochondria and uncoupling eNOS(Kashihara et al., 2010). ROS overproduction induces glomerular cell proliferation and activates redox-sensitive NF-κB to initiate an inflammatory cascade in the kidney, persistent renal inflammation and chronic oxidative

stress may damage renal structural and function(Li et al., 2022; Malik et al., 2017). In this study, we show that increased ROS generation is associated with a decrease in antioxidant genes GPX_4 and NRF_2 expression in the kidney of diabetes mice, atorvastatin significantly reduces renal ROS and increases the expression of antioxidant genes.

The death of renal tubular cells is considered to be an early event and a major cause of proteinuria in the patients with DKD(Phillips and Steadman, 2002). Many factors, including ROS, ischemia and inflammatory cytokines, contribute to renal tubular cell death(Pesce et al., 2002; Qiu et al., 2022). Recent studies suggest that ferroptosis is one of the main causes of renal tubular cell death in diabetes(Tan et al., 2022). Ferroptosis is characterized with the loss of the antioxidant capability and the accumulation of redox-active iron and lipid peroxidation products(Hadian and Stockwell, 2020). The loss of activities of antioxidant enzymes GPX_4, NRF_2 as well as the depletion of glutathione, are considered the main causes of ferroptosis(Ursini and Maiorino, 2020). It has been shown that erastin induces ferroptosis though the depletion of GPX_4(Imai et al., 2017). NRF_2 is a transcription factor that not only regulates the expression of antioxidant genes but also regulates the genes of iron metabolism(Dodson et al., 2019). In diabetes, hyperglycemia and hyperlipidemia increase renal oxidative stress and lower the antioxidant capacity of GPX_4 and NRF_2, resulting in an oxidative-redox imbalance and abnormal iron accumulation(Chen et al., 2022; Zhang et al., 2022b). The overload of redox-active iron further increases ROS generation through Fenton reaction, which promotes lipid oxidation and the generation of lipid peroxide products, leading to ferroptotic cell death in renal cells, especially tubular cells(Martines et al., 2013; Pan et al., 2022).

Although it is well demonstrated that statins therapy can provide beneficial effects in cardiovascular diseases and diabetes mellitus(Ning et al., 2021; Taylor et al., 2017), whether statins can inhibit ferroptosis is still controversial. Liu et al showed that atorvastatin inhibited cardiac

ferroptosis and inflammation and ameliorated coronary microembolization-induced myocardia injury (Liu et al., 2022). In contrast, Zhang et al reported that statins could increase intracellular accumulation of ROS, iron and lipid peroxide products, lowered the antioxidant capacity of GPX_4 and NRF_2, and promoted ferroptosis in cardiomyocytes and skeletal muscle cells(Zhang et al., 2022a). The discrepancy of statins effects on ferroptosis may depend on cell type, the dose and different kinds of statins used(Climent et al., 2019). As far, there are no publications showing whether statins can inhibit renal ferroptosis in DKD mice. In this study, DKD mice exhibits renal iron accumulation, increased ROS, FTH and iron oxidative lipid damage products MDA and 4HNE, and decreased GPX_4, NRF_2 and TFR1. These change in ferroptosis-related signaling molecules can also be observed in HK_2 cells treated with high glucose or erastin. In addition, erastin or high glucose causes characteristic changes of ferroptosis in mitochondrial morphology. Atorvastatin reverses these changes in ferroptosis signaling molecule in diabetes mice and in high glucose or erastin treated HK2 cells. These results suggest statins can inhibit renal ferroptosis signaling in DKD mice.

It is well known that ferroptosis is an oxidative, iron-dependent form of cell death, which is triggered by loss of cellular glutathione-dependent antioxidant capacity and accumulation of toxic lipid ROS (Dixon et al., 2012). To elucidate the relationship between atorvastatin's antioxidant and its inhibition of ferroptosis signaling, we compare the effect of atorvastatin, ferroptosis inhibitor ferrostatin-1, antioxidant NAC on ROS formation and ferroptosis signaling in high glucose-treated HK_2 cells. Atorvastatin, ferrostatin-1, and NAC have the same inhibitory effect on high glucose-induced ROS generation, and both NAC and ferrostatin-1 have almost the same inhibitory effect on high glucose-induced ferroptosis signaling. These results suggest that high glucose promotes ferroptosis signaling mainly by increasing ROS generation in renal tubular cells, and atorvastatin may inhibit high glucose-induced ferroptosis signaling by reducing ROS formation.

This study has some limitations. First, atorvastatin significantly reduces lipid profile in diabetes mice, it has been reported that hyperlipidemia may induce ferroptosis (Kuang et al., 2023), thus it can't be ruled out that atorvastatin inhibition of renal ferroptosis may be partially caused by its lipid-lowering effects. Next, atorvastatin can prevent high glucose-induced iron accumulation and reduction in cell viability, reverse ferroptosis-related protein expression and mitochondrial abnormalities in HK_2 cells. Although atorvastatin inhibits renal ferroptosis signaling, this study does not provide direct evidence that atorvastatin can inhibit renal cell death in diabetes mice. Finally, we used DHE fluorescence dye to measure renal ROS production. Although this method is widely used for measuring tissue ROS, DHE may also produce red fluorescence through nonspecific oxidation processes, not solely due to ROS (Kalyanaraman et al., 2014).

In summary, we have demonstrated that atorvastatin reduces renal injury and ROS formation, and improves ferroptosis signaling in diabetes mice. Atorvastatin also inhibits hyperglycemia- or erastin-induced ROS formation, and improves hyperglycemia- or erastin-induced mitochondria injury and ferroptosis signaling in renal tubular cells *in vitro*. The mechanisms by which atorvastatin inhibits ferroptosis signaling may be mediated by antioxidant effects. The inhibition of ferroptosis signaling pathway may represent a new mechanism for statins protection of renal injury in DKD patients.

Declaration of competing interest

All authors declare that the work was conducted in the absence of any commercial or financial relationships that could be construed as a potential conflict of interest.

Data availability

The original contributions presented in the study are included in the article/Supplementary Materials, further inquiries can be directed to the corresponding authors.

Acknowledgements

This work was funded by the National Natural Science Foundation of China (Nos. 81970357, 2019; 82270434, 2022) to Ming-Sheng Zhou, and National Natural Science Foundation of China (82100316), the Doctoral Scientific Research Foundation of Liaoning Province (2022-BS-342) to Lu Zhang.

Author contributions

YZ contributed to experimental design; animal experiment and statistical analysis. YQ contributed to animal study and cell experiment; RC contributed to data acquisition, statistical analysis; QX contributed to animal experiments; LZ, MK and JG contributed to cell experiments; QC and YL contributed to pathological experiments; FR contributed to experimental design and data explanation; MSZ contributed to the conception and design of the work, data interpretation and manuscript draft and revision.

References:

Ayala, A., Munoz, M.F., Arguelles, S., 2014. Lipid peroxidation: production, metabolism, and signaling mechanisms of malondialdehyde and 4-hydroxy-2-nonenal. Oxid Med Cell Longev 2014, 360438. https://doi.10.1155/2014/360438

Baigent, C., Landray, M.J., Reith, C., Emberson, J., Wheeler, D.C., Tomson, C., Wanner, C., Krane, V., Cass, A., Craig, J., Neal, B., Jiang, L., Hooi, L.S., Levin, A., Agodoa, L., Gaziano, M., Kasiske, B., Walker, R., Massy, Z.A., Feldt-Rasmussen, B., Krairittichai, U., Ophascharoensuk, V., Fellstrom, B., Holdaas, H., Tesar, V., Wiecek, A., Grobbee, D., de Zeeuw, D., Gronhagen-Riska, C., Dasgupta, T., Lewis, D., Herrington, W., Mafham, M., Majoni, W., Wallendszus, K., Grimm, R., Pedersen, T., Tobert, J., Armitage, J., Baxter, A., Bray, C., Chen, Y., Chen, Z., Hill,

M., Knott, C., Parish, S., Simpson, D., Sleight, P., Young, A., Collins, R., Investigators, S., 2011. The effects of lowering LDL cholesterol with simvastatin plus ezetimibe in patients with chronic kidney disease (Study of Heart and Renal Protection): a randomised placebo-controlled trial. Lancet 377, 2181-2192. https://doi.10.1016/S0140-6736(11)60739-3

Barayev, O., Hawley, C.E., Wellman, H., Gerlovin, H., Hsu, W., Paik, J.M., Mandel, E.I., Liu, C.K., Djousse, L., Gaziano, J.M., Gagnon, D.R., Orkaby, A.R., 2023. Statins, Mortality, and Major Adverse Cardiovascular Events Among US Veterans With Chronic Kidney Disease. JAMA Netw Open 6, e2346373. https://doi.10.1001/jamanetworkopen.2023.46373

Battisti, W.P., Palmisano, J., Keane, W.E., 2003. Dyslipidemia in patients with type 2 diabetes. relationships between lipids, kidney disease and cardiovascular disease. Clin Chem Lab Med 41, 1174-1181. https://doi.10.1515/CCLM.2003.181

Bellosta, S., Ferri, N., Bernini, F., Paoletti, R., Corsini, A., 2000. Non-lipid-related effects of statins. Ann Med 32, 164-176. https://doi.10.3109/07853890008998823

Bolignano, D., Cernaro, V., Gembillo, G., Baggetta, R., Buemi, M., D'Arrigo, G., 2017. Antioxidant agents for delaying diabetic kidney disease progression: A systematic review and meta-analysis. PLoS One 12, e0178699. https://doi.10.1371/journal.pone.0178699

Chen, J., Ou, Z., Gao, T., Yang, Y., Shu, A., Xu, H., Chen, Y., Lv, Z., 2022. Ginkgolide B alleviates oxidative stress and ferroptosis by inhibiting GPX4 ubiquitination to improve diabetic nephropathy. Biomed Pharmacother 156, 113953. https://doi.10.1016/j.biopha.2022.113953

Chen, S.C., Tseng, C.H., 2013. Dyslipidemia, kidney disease, and cardiovascular disease in diabetic patients. Rev Diabet Stud 10, 88-100. https://doi.10.1900/RDS.2013.10.88

Chen, Y., Huang, G., Qin, T., Zhang, Z., Wang, H., Xu, Y., Shen, X., 2024. Ferroptosis: A new view on the prevention and treatment of diabetic kidney disease with traditional Chinese medicine. Biomed Pharmacother 170, 115952. https://doi.10.1016/j.biopha.2023.115952

Cholesterol Treatment Trialists, C., Herrington, W.G., Emberson, J., Mihaylova, B., Blackwell, L., Reith, C., Solbu, M.D., Mark, P.B., Fellstrom, B., Jardine, A.G., Wanner, C., Holdaas, H., Fulcher, J., Haynes, R., Landray, M.J., Keech, A., Simes, J., Collins, R., Baigent, C., 2016. Impact of renal function on the effects of LDL cholesterol lowering with statin-based regimens: a meta-analysis of individual participant data from 28 randomised trials. Lancet Diabetes Endocrinol 4, 829-839. https://doi.10.1016/S2213-8587(16)30156-5

Climent, E., Benaiges, D., Pedro-Botet, J., 2019. Statin treatment and increased diabetes risk. Possible mechanisms. Clin Investig Arterioscler 31, 228-232. https://doi.10.1016/j.arteri.2018.12.001

Colhoun, H.M., Betteridge, D.J., Durrington, P.N., Hitman, G.A., Neil, H.A., Livingstone, S.J., Charlton-Menys, V., DeMicco, D.A., Fuller, J.H., Investigators, C., 2009. Effects of atorvastatin on kidney outcomes and cardiovascular disease in patients with diabetes: an analysis from the Collaborative Atorvastatin Diabetes Study (CARDS). Am J Kidney Dis 54, 810-819. https://doi.10.1053/j.ajkd.2009.03.022

Deng, J., Wu, G., Yang, C., Li, Y., Jing, Q., Han, Y., 2015. Rosuvastatin attenuates contrast-induced nephropathy through modulation of nitric oxide, inflammatory responses, oxidative stress and apoptosis in diabetic male rats. J Transl Med 13, 53. https://doi.10.1186/s12967-015-0416-1

600 Dixon, S.J., Lemberg, K.M., Lamprecht, M.R., Skouta, R., Zaitsev, E.M., Gleason, C.E., Patel, D.N.,
601 Bauer, A.J., Cantley, A.M., Yang, W.S., Morrison, B., 3rd, Stockwell, B.R., 2012. Ferroptosis:
602 an iron-dependent form of nonapoptotic cell death. Cell 149, 1060-1072.
603 https://doi.10.1016/j.cell.2012.03.042
604 Dodson, M., Castro-Portuguez, R., Zhang, D.D., 2019. NRF2 plays a critical role in mitigating lipid
605 peroxidation and ferroptosis. Redox Biol 23, 101107.
606 https://doi.10.1016/j.redox.2019.101107
607 Feng, X., Wang, S., Sun, Z., Dong, H., Yu, H., Huang, M., Gao, X., 2021. Ferroptosis Enhanced
608 Diabetic Renal Tubular Injury via HIF-1alpha/HO-1 Pathway in db/db Mice. Front Endocrinol
609 (Lausanne) 12, 626390. https://doi.10.3389/fendo.2021.626390
610 Gao, G., Li, J., Zhang, Y., Chang, Y.Z., 2019. Cellular Iron Metabolism and Regulation. Adv Exp
611 Med Biol 1173, 21-32. https://doi.10.1007/978-981-13-9589-5_2
612 Gaschler, M.M., Andia, A.A., Liu, H., Csuka, J.M., Hurlocker, B., Vaiana, C.A., Heindel, D.W.,
613 Zuckerman, D.S., Bos, P.H., Reznik, E., Ye, L.F., Tyurina, Y.Y., Lin, A.J., Shchepinov, M.S.,
614 Chan, A.Y., Peguero-Pereira, E., Fomich, M.A., Daniels, J.D., Bekish, A.V., Shmanai, V.V.,
615 Kagan, V.E., Mahal, L.K., Woerpel, K.A., Stockwell, B.R., 2018. FINO(2) initiates ferroptosis
616 through GPX4 inactivation and iron oxidation. Nat Chem Biol 14, 507-515.
617 https://doi.10.1038/s41589-018-0031-6
618 Gruden, G., Perin, P.C., Camussi, G., 2005. Insight on the pathogenesis of diabetic nephropathy
619 from the study of podocyte and mesangial cell biology. Curr Diabetes Rev 1, 27-40.
620 https://doi.10.2174/1573399052952622
621 Hadian, K., Stockwell, B.R., 2020. SnapShot: Ferroptosis. Cell 181, 1188-1188 e1181.
622 https://doi.10.1016/j.cell.2020.04.039
623 Huang, L., Wang, A., Hao, Y., Li, W., Liu, C., Yang, Z., Zheng, F., Zhou, M.S., 2018. Macrophage
624 Depletion Lowered Blood Pressure and Attenuated Hypertensive Renal Injury and Fibrosis.
625 Front Physiol 9, 473. https://doi.10.3389/fphys.2018.00473
626 Huang, T.S., Wu, T., Wu, Y.D., Li, X.H., Tan, J., Shen, C.H., Xiong, S.J., Feng, Z.Q., Gao, S.F., Li, H.,
627 Cai, W.B., 2023. Long-term statins administration exacerbates diabetic nephropathy via
628 ectopic fat deposition in diabetic mice. Nat Commun 14, 390. https://doi.10.1038/s41467-
629 023-35944-z
630 Huang, Y., Yuan, X., 2024. Novel ferroptosis gene biomarkers and immune infiltration profiles in
631 diabetic kidney disease via bioinformatics. FASEB J 38, e23421.
632 https://doi.10.1096/fj.202301357RR
633 Imai, H., Matsuoka, M., Kumagai, T., Sakamoto, T., Koumura, T., 2017. Lipid Peroxidation-
634 Dependent Cell Death Regulated by GPx4 and Ferroptosis. Curr Top Microbiol Immunol
635 403, 143-170. https://doi.10.1007/82_2016_508
636 Kalyanaraman, B., Dranka, B.P., Hardy, M., Michalski, R., Zielonka, J., 2014. HPLC-based
637 monitoring of products formed from hydroethidine-based fluorogenic probes--the ultimate
638 approach for intra- and extracellular superoxide detection. Biochimica et biophysica acta
639 1840, 739-744. https://doi.10.1016/j.bbagen.2013.05.008
640 Kashihara, N., Haruna, Y., Kondeti, V.K., Kanwar, Y.S., 2010. Oxidative stress in diabetic
641 nephropathy. Curr Med Chem 17, 4256-4269. https://doi.10.2174/092986710793348581
642 Kuang, H., Sun, X., Liu, Y., Tang, M., Wei, Y., Shi, Y., Li, R., Xiao, G., Kang, J., Wang, F., Peng, J., Xu,
643 H., Zhou, F., 2023. Palmitic acid-induced ferroptosis via CD36 activates ER stress to break

calcium-iron balance in colon cancer cells. FEBS J 290, 3664-3687. https://doi.10.1111/febs.16772

Li, J., Cao, F., Yin, H.L., Huang, Z.J., Lin, Z.T., Mao, N., Sun, B., Wang, G., 2020. Ferroptosis: past, present and future. Cell Death Dis 11, 88. https://doi.10.1038/s41419-020-2298-2

Li, Y., Ou, S., Liu, Q., Gan, L., Zhang, L., Wang, Y., Qin, J., Liu, J., Wu, W., 2022. Genistein improves mitochondrial function and inflammatory in rats with diabetic nephropathy via inhibiting MAPK/NF-kappaB pathway. Acta Cir Bras 37, e370601. https://doi.10.1590/acb370601

Liao, T., Xu, X., Ye, X., Yan, J., 2022. DJ-1 upregulates the Nrf2/GPX4 signal pathway to inhibit trophoblast ferroptosis in the pathogenesis of preeclampsia. Sci Rep 12, 2934. https://doi.10.1038/s41598-022-07065-y

Lindblom, R., Higgins, G., Coughlan, M., de Haan, J.B., 2015. Targeting Mitochondria and Reactive Oxygen Species-Driven Pathogenesis in Diabetic Nephropathy. Rev Diabet Stud 12, 134-156. https://doi.10.1900/RDS.2015.12.134

Liu, T., Shu, J., Liu, Y., Xie, J., Li, T., Li, H., Li, L., 2022. Atorvastatin attenuates ferroptosis-dependent myocardial injury and inflammation following coronary microembolization via the Hif1a/Ptgs2 pathway. Front Pharmacol 13, 1057583. https://doi.10.3389/fphar.2022.1057583

Malik, S., Suchal, K., Khan, S.I., Bhatia, J., Kishore, K., Dinda, A.K., Arya, D.S., 2017. Apigenin ameliorates streptozotocin-induced diabetic nephropathy in rats via MAPK-NF-kappaB-TNF-alpha and TGF-beta1-MAPK-fibronectin pathways. Am J Physiol Renal Physiol 313, F414-F422. https://doi.10.1152/ajprenal.00393.2016

Mansi, I.A., Chansard, M., Lingvay, I., Zhang, S., Halm, E.A., Alvarez, C.A., 2021. Association of Statin Therapy Initiation With Diabetes Progression: A Retrospective Matched-Cohort Study. JAMA Intern Med 181, 1562-1574. https://doi.10.1001/jamainternmed.2021.5714

Martines, A.M., Masereeuw, R., Tjalsma, H., Hoenderop, J.G., Wetzels, J.F., Swinkels, D.W., 2013. Iron metabolism in the pathogenesis of iron-induced kidney injury. Nat Rev Nephrol 9, 385-398. https://doi.10.1038/nrneph.2013.98

Mengstie, M.A., Seid, M.A., Gebeyehu, N.A., Adella, G.A., Kassie, G.A., Bayih, W.A., Gesese, M.M., Anley, D.T., Feleke, S.F., Zemene, M.A., Dessie, A.M., Solomon, Y., Bantie, B., Dejenie, T.A., Teshome, A.A., Abebe, E.C., 2023. Ferroptosis in diabetic nephropathy: Mechanisms and therapeutic implications. Metabol Open 18, 100243. https://doi.10.1016/j.metop.2023.100243

Ning, D., Yang, X., Wang, T., Jiang, Q., Yu, J., Wang, D., 2021. Atorvastatin treatment ameliorates cardiac function and remodeling induced by isoproterenol attack through mitigation of ferroptosis. Biochem Biophys Res Commun 574, 39-47. https://doi.10.1016/j.bbrc.2021.08.017

Orkaby, A.R., Driver, J.A., Ho, Y.L., Lu, B., Costa, L., Honerlaw, J., Galloway, A., Vassy, J.L., Forman, D.E., Gaziano, J.M., Gagnon, D.R., Wilson, P.W.F., Cho, K., Djousse, L., 2020. Association of Statin Use With All-Cause and Cardiovascular Mortality in US Veterans 75 Years and Older. JAMA 324, 68-78. https://doi.10.1001/jama.2020.7848

Ostergaard, J.A., Cooper, M.E., Jandeleit-Dahm, K.A.M., 2020. Targeting oxidative stress and anti-oxidant defence in diabetic kidney disease. J Nephrol 33, 917-929. https://doi.10.1007/s40620-020-00749-6

687 Pan, Z., He, Q., Zeng, J., Li, S., Li, M., Chen, B., Yang, J., Xiao, J., Zeng, C., Luo, H., Wang, H., 2022.
688 Naringenin protects against iron overload-induced osteoarthritis by suppressing oxidative
689 stress. Phytomedicine 105, 154330. https://doi.10.1016/j.phymed.2022.154330
690 Pesce, C., Menini, S., Pricci, F., Favre, A., Leto, G., DiMario, U., Pugliese, G., 2002. Glomerular cell
691 replication and cell loss through apoptosis in experimental diabetes mellitus. Nephron 90,
692 484-488. https://doi.10.1159/000054738
693 Phillips, A.O., Steadman, R., 2002. Diabetic nephropathy: the central role of renal proximal
694 tubular cells in tubulointerstitial injury. Histol Histopathol 17, 247-252.
695 https://doi.10.14670/HH-17.247
696 Qin, X., Dong, H., Fang, K., Lu, F., 2017. The effect of statins on renal outcomes in patients with
697 diabetic kidney disease: A systematic review and meta-analysis. Diabetes Metab Res Rev
698 33. https://doi.10.1002/dmrr.2901
699 Qiu, D., Song, S., Wang, Y., Bian, Y., Wu, M., Wu, H., Shi, Y., Duan, H., 2022. NAD(P)H: quinone
700 oxidoreductase 1 attenuates oxidative stress and apoptosis by regulating Sirt1 in diabetic
701 nephropathy. J Transl Med 20, 44. https://doi.10.1186/s12967-021-03197-3
702 Rochette, L., Dogon, G., Rigal, E., Zeller, M., Cottin, Y., Vergely, C., 2022. Lipid Peroxidation and
703 Iron Metabolism: Two Corner Stones in the Homeostasis Control of Ferroptosis. Int J Mol
704 Sci 24. https://doi.10.3390/ijms24010449
705 Samsu, N., 2021. Diabetic Nephropathy: Challenges in Pathogenesis, Diagnosis, and Treatment.
706 Biomed Res Int 2021, 1497449. https://doi.10.1155/2021/1497449
707 Sandhu, S., Wiebe, N., Fried, L.F., Tonelli, M., 2006. Statins for improving renal outcomes: a
708 meta-analysis. J Am Soc Nephrol 17, 2006-2016. https://doi.10.1681/ASN.2006010012
709 Shen, S., Ji, C., Wei, K., 2022. Cellular Senescence and Regulated Cell Death of Tubular Epithelial
710 Cells in Diabetic Kidney Disease. Front Endocrinol (Lausanne) 13, 924299.
711 https://doi.10.3389/fendo.2022.924299
712 Shen, X., Zhang, Z., Zhang, X., Zhao, J., Zhou, X., Xu, Q., Shang, H., Dong, J., Liao, L., 2016. Efficacy
713 of statins in patients with diabetic nephropathy: a meta-analysis of randomized controlled
714 trials. Lipids Health Dis 15, 179. https://doi.10.1186/s12944-016-0350-0
715 Tan, H., Chen, J., Li, Y., Li, Y., Zhong, Y., Li, G., Liu, L., Li, Y., 2022. Glabridin, a bioactive
716 component of licorice, ameliorates diabetic nephropathy by regulating ferroptosis and the
717 VEGF/Akt/ERK pathways. Mol Med 28, 58. https://doi.10.1186/s10020-022-00481-w
718 Taylor, B.A., Ng, J., Stone, A., Thompson, P.D., Papasavas, P.K., Tishler, D.S., 2017. Effects of
719 statin therapy on weight loss and diabetes in bariatric patients. Surg Obes Relat Dis 13,
720 674-680. https://doi.10.1016/j.soard.2016.11.018
721 Ursini, F., Maiorino, M., 2020. Lipid peroxidation and ferroptosis: The role of GSH and GPx4.
722 Free Radic Biol Med 152, 175-185. https://doi.10.1016/j.freeradbiomed.2020.02.027
723 Winiarska, A., Knysak, M., Nabrdalik, K., Gumprecht, J., Stompor, T., 2021. Inflammation and
724 Oxidative Stress in Diabetic Kidney Disease: The Targets for SGLT2 Inhibitors and GLP-1
725 Receptor Agonists. Int J Mol Sci 22. https://doi.10.3390/ijms221910822
726 Wu, K., Fei, L., Wang, X., Lei, Y., Yu, L., Xu, W., Chen, J., Zhu, E., Zhong, M., Huang, M., Xi, J., Yin,
727 F., Yan, Z., Zhao, X., Tang, C., Patzak, A., Liu, X., Zheng, Z., 2022. ZIP14 is involved in iron
728 deposition and triggers ferroptosis in diabetic nephropathy. Metallomics 14.
729 https://doi.10.1093/mtomcs/mfac034

Xu, S., Wu, B., Zhong, B., Lin, L., Ding, Y., Jin, X., Huang, Z., Lin, M., Wu, H., Xu, D., 2021. Naringenin alleviates myocardial ischemia/reperfusion injury by regulating the nuclear factor-erythroid factor 2-related factor 2 (Nrf2) /System xc-/ glutathione peroxidase 4 (GPX4) axis to inhibit ferroptosis. Bioengineered 12, 10924-10934. https://doi.10.1080/21655979.2021.1995994

Zhang, Q., Qu, H., Chen, Y., Luo, X., Chen, C., Xiao, B., Ding, X., Zhao, P., Lu, Y., Chen, A.F., Yu, Y., 2022a. Atorvastatin Induces Mitochondria-Dependent Ferroptosis via the Modulation of Nrf2-xCT/GPx4 Axis. Front Cell Dev Biol 10, 806081. https://doi.10.3389/fcell.2022.806081

Zhang, X., Xing, L., Jia, X., Pang, X., Xiang, Q., Zhao, X., Ma, L., Liu, Z., Hu, K., Wang, Z., Cui, Y., 2020. Comparative Lipid-Lowering/Increasing Efficacy of 7 Statins in Patients with Dyslipidemia, Cardiovascular Diseases, or Diabetes Mellitus: Systematic Review and Network Meta-Analyses of 50 Randomized Controlled Trials. Cardiovasc Ther 2020, 3987065. https://doi.10.1155/2020/3987065

Zhang, Y., Wu, Q., Liu, J., Zhang, Z., Ma, X., Zhang, Y., Zhu, J., Thring, R.W., Wu, M., Gao, Y., Tong, H., 2022b. Sulforaphane alleviates high fat diet-induced insulin resistance via AMPK/Nrf2/GPx4 axis. Biomed Pharmacother 152, 113273. https://doi.10.1016/j.biopha.2022.113273

Zhou, M.S., Schuman, I.H., Jaimes, E.A., Raij, L., 2008. Renoprotection by statins is linked to a decrease in renal oxidative stress, TGF-beta, and fibronectin with concomitant increase in nitric oxide bioavailability. Am J Physiol Renal Physiol 295, F53-59. https://doi.10.1152/ajprenal.00041.2008

Zhou, S., Zhao, P., Li, Y., Deng, T., Tian, L., Li, H., 2014. Renoprotective effect of atorvastatin on STZ-diabetic rats through attenuating kidney-associated dysmetabolism. Eur J Pharmacol 740, 9-14. https://doi.10.1016/j.ejphar.2014.06.055

Zigmont, V.A., Shoben, A.B., Lu, B., Kaye, G.L., Clinton, S.K., Harris, R.E., Olivo-Marston, S.E., 2019. Statin users have an elevated risk of dysglycemia and new-onset-diabetes. Diabetes Metab Res Rev 35, e3189. https://doi.10.1002/dmrr.3189

Declaration of interests

The authors declare that they have no known competing financial interests or personal relationships that could have appeared to influence the work reported in this paper.